Learning-Based Building Flexibility Estimation and Control to Improve Microgrid Economics and Resilience

Preprint

Fei Ding,[1] Yiyun Yao,[1] Jun Hao,[1] Yansong Pei,[2]
Jiyu Wang,[1] and Junbo Zhao[2]

1 National Renewable Energy Laboratory
2 University of Connecticut

Presented at the 2024 IEEE Power and Energy Society General Meeting
Seattle, Washington
July 21–25, 2024

NREL is a national laboratory of the U.S. Department of Energy
Office of Energy Efficiency & Renewable Energy
Operated by the Alliance for Sustainable Energy, LLC

This report is available at no cost from the National Renewable Energy Laboratory (NREL) at www.nrel.gov/publications.

Contract No. DE-AC36-08GO28308

Conference Paper
NREL/CP-5D00-89331
July 2024

Learning-Based Building Flexibility Estimation and Control to Improve Microgrid Economics and Resilience

Preprint

Fei Ding,[1] Yiyun Yao,[1] Jun Hao,[1] Yansong Pei,[2]
Jiyu Wang,[1] and Junbo Zhao[2]

1 National Renewable Energy Laboratory
2 University of Connecticut

Suggested Citation
Ding, Fei, Yiyun Yao, Jun Hao, Yansong Pei, Jiyu Wang, and Junbo Zhao. 2024. *Learning-Based Building Flexibility Estimation and Control to Improve Microgrid Economics and Resilience: Preprint*. Golden, CO: National Renewable Energy Laboratory. NREL/CP-5D00-89331. https://www.nrel.gov/docs/fy24osti/89331.pdf.

NREL is a national laboratory of the U.S. Department of Energy
Office of Energy Efficiency & Renewable Energy
Operated by the Alliance for Sustainable Energy, LLC

This report is available at no cost from the National Renewable Energy Laboratory (NREL) at www.nrel.gov/publications.

Contract No. DE-AC36-08GO28308

Conference Paper
NREL/CP-5D00-89331
July 2024

National Renewable Energy Laboratory
15013 Denver West Parkway
Golden, CO 80401
303-275-3000 • www.nrel.gov

NOTICE

This work was authored in part by the National Renewable Energy Laboratory, operated by Alliance for Sustainable Energy, LLC, for the U.S. Department of Energy (DOE) under Contract No. DE-AC36-08GO28308. Funding provided by the U.S. Department of Defense (DOD) the Environmental Security Technology Certification Program (ESTCP), Agreement Number EW22-7467. The views expressed herein do not necessarily represent the views of the DOE or the U.S. Government.

Cover Photos by Dennis Schroeder: (clockwise, left to right) NREL 51934, NREL 45897, NREL 42160, NREL 45891, NREL 48097, NREL 46526.

Learning-Based Building Flexibility Estimation and Control to Improve Microgrid Economics and Resilience

Fei Ding[1], *Senior Member, IEEE*, Yiyun Yao[1], *Member, IEEE*, Jun Hao[1], *Member, IEEE*, Yansong Pei[2], *Student Member, IEEE*, Jiyu Wang[1], *Member, IEEE*, Junbo Zhao[2], *Senior Member, IEEE*

[1]National Renewable Energy Laboratory, 10513 Denver W Pkwy, Golden, CO 80401
[2]University of Connecticut, 2131 Hillside Road, Unit 3088 Storrs, CT 06269

***Abstract*—This paper proposes a learning-based building flexibility estimation and control framework to improve system economics and resilience. A data-driven building load flexibility model consisting of weather forecasting and estimating load consumption is proposed to quantify building heating, ventilation, and air conditioning (HVAC) load flexibility. A reinforcement learning-based microgrid controller is proposed to dispatch distributed generators, distributed energy resources, and build HVAC loads while taking flexibility information as one of the inputs. Simulation analysis is conducted on the model of a real microgrid in California. The effectiveness of the proposed learning-based building flexibility estimation and control in reducing microgrid energy costs and improving the sustainability of critical loads is demonstrated.**

***Index Terms*—Microgrid, building load flexibility, reinforcement learning, resilience.**

I. Introduction

Critical facilities rely on distributed generation and microgrids to provide power support for critical loads under utility grid outages. To achieve resilient and secure operations, harnessing demand-side flexibility and optimally coordinating building operations with other distributed energy resources (DERs) is also indispensable. To realize scalable load management, two challenges need to be addressed: 1) Quantitative understanding of load flexibility to improve energy resilience: Major building loads, such as air conditioners, are schedulable, and non-critical building loads are interruptible. Thus, optimal operation of these controllable building loads could provide additional flexibility that can be dispatched together with other DERs to maximize the power supply redundancy for fulfilling the needs of critical loads. Although some methods have been developed to quantify load flexibility [1], these methods are not designed for critical load management during islanding events. 2) Requirement of computationally efficient optimization approach: Proactive and adaptive decision-making is important to improve system resilience. However, traditional model-based approaches [2], [3] usually rely on solving complex, centralized optimization problems, which require heavy computation efforts and might not be scalable for real-time applications. Incorporating machine learning techniques into building load management and microgrid optimization is envisioned to be a promising solution. Although learning-based building controls have been studied a lot, such as [4]-[5], this paper differentiates from all other works by first integrating quantified building flexibility into control, and secondly exploring the value of flexibility in improving energy efficiency and resilience for realistic microgrid systems with hundreds of buildings and other on-site energy resources. This paper introduces a novel approach to microgrid management by integrating demand-side flexibility and advanced reinforcement learning techniques, enabling a quantitatively precise and computationally efficient control of building loads. This innovative method significantly enhances energy efficiency and resilience in critical facilities, particularly during grid outages, by effectively coordinating numerous buildings and diverse onsite energy resources.

This work was authored in part by the National Renewable Energy Laboratory, operated by Alliance for Sustainable Energy, LLC, for the U.S. Department of Energy (DOE) under Contract No. DE-AC36-08GO28308. Funding provided by the U.S. Department of Defense (DOD) the Environmental Security Technology Certification Program (ESTCP), Agreement Number EW22-7467. The views expressed in the article do not necessarily represent the views of the DOE or the U.S. Government. The U.S. Government retains and the publisher, by accepting the article for publication, acknowledges that the U.S. Government retains a nonexclusive, paid-up, irrevocable, worldwide license to publish or reproduce the published form of this work, or allow others to do so, for U.S. Government purposes.

II. Data-Driven Building Load Flexibility Estimation

In this paper, we propose a data-driven model to estimate building HVAC load flexibility. As shown in Fig. 1, the proposed model consists of two parts, including weather forecasting module and consumption estimation module.

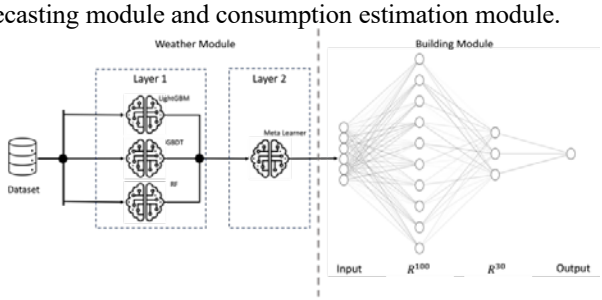

Fig. 1. The proposed hybrid module.

HVAC load consumption is affected by weather condition and building features. After conducting a linear correlation analysis, we identified five features as the inputs to train the weather forecasting neural network, which are outside dry-bulb temperature, HVAC cooling setpoint, HVAC heating setpoint, site diffuse solar radiation rate per area, and site direct solar radiation rate per area. Thus, the weather forecasting module will forecast outside temperature and solar radiation, and the forecasted information will be used as the inputs for the HVAC consumption module. Taking outside dry-bulb temperature as an example, as shown in Fig.1, the weather module is a two-layer stacking model based on ensemble methods. The input of the weather module is a time-series of d-dimensional observations,

$x_t, \dots, x_{t'} \in \mathbb{R}^d$ that starts at time step t and end at time step t'. The outputs are the estimations of future multi-horizon outside dry-bulb temperature at a site-specific location $\hat{y}_{(t'+1):(t'+h)} \in \mathbb{R}^h$ given the observations $\boldsymbol{X} \in \mathbb{R}^d$,where h is the number of time stamps to be estimated. The first layer consists of three ensemble methods including random forest (RF), Gradient-boosted decision tree (GBDT), and LightGBM. Thus, the mapping of inputs and outputs of the first layer can be:

$$r(x_t, \dots, x_{t'}) = L^r(y_{(t'+1):(t'+H)} - \hat{y}^r{}_{(t'+1):(t'+H)}) \quad (1)$$

$$g(x_t, \dots, x_{t'}) = L^g(y_{(t'+1):(t'+H)} - \hat{y}^g{}_{(t'+1):(t'+H)}) \quad (2)$$

$$b(x_t, \dots, x_{t'}) = L^b(y_{(t'+1):(t'+H)} - \hat{y}^b{}_{(t'+1):(t'+H)}) \quad (3)$$

where r, g, b are the function of RF, GBDT, and LightGBM, respectively, and L^r, L^g, L^b are the corresponding loss functions. For the second layer in the weather module, the goal is to assign weights to the outputs of the first layer, assume the weights of each base learner in first layers are w_r, w_g, and w_b for r, g, b, and $w_r, w_g, w_b \in (0,1)$. The output of the second layer can be:

$$\hat{y}_{(t'+1):(t'+h)} = w_r * \hat{y}^r + w_g * \hat{y}^g + w_b * \hat{y}^b \quad (4)$$

The consumption module is responsible for estimating the HVAC power consumption at a given weather condition and an indoor temperature setting. It is designed as a multiplayer feedforward artificial neural network (ANN), which has one input layer, three hidden layers, and one output layer. Let p_i define the estimation of HVAC power consumption at time stamp i, and $\boldsymbol{e}_i \in \mathbb{R}$ be the input of the proposed ANN at a given time i. The input and output can be expressed as a function of $p_i = g(\boldsymbol{e}_i)$. Among the input features in $\boldsymbol{e}_i$, let s_i define the indoor temperature setting, and $\boldsymbol{r}_i$ define the rest environmental features. At a given time t, $\boldsymbol{r}_i$ is fixed, and the only variable will be s_i. Let s_l define the lower bound of the temperature setting, and s_u define the upper bound of the temperature setting, we can have $s_l \le s_i \le s_u$. By setting s_i, the flexibility of a HVAC system can be expressed as $p_l \le p_i \le p_m$, where p_l and p_u define the lower and upper bounds at time t.

III. Flexibility-Informed, Reinforcement Learning Based Microgrid Control

A. Overall Structure

In this paper, the control problem is designed to address the objectives of both normal grid-connected operation and islanded microgrid operation. To formulate the problem, let us denote discrete steps $t \in T = \{1, \dots, T\}$. The controllable DERs include PV ($\mathcal{H}$), battery ($\mathcal{B}$), and fuel-based generator ($\mathcal{D}$), flexible HVAC load ($\mathcal{FH}$) and all together denoted as $\mathcal{G} = \mathcal{H} \cup \mathcal{B} \cup \mathcal{D} \cup \mathcal{FH}$. At each time step t, the microgrid control agent determines the power setpoints for all controllable DERs (i.e., $p_t^{\mathcal{G}}, q_t^{\mathcal{G}}$) and the value of supplied load (i.e., $p_t^{\mathcal{L}}, q_t^{\mathcal{L}}$) to achieve predefined operational goal and satisfy the system as well as DER operational security constraints. Let $x_t := (p_t^{\mathcal{G}}, q_t^{\mathcal{G}})$, the microgrid control problem can be formulated as a classic optimal power flow (OPF) problem, as:

$$max_{x_t}: \quad \sum_{t \in \mathcal{T}} f(x_t) \quad (5)$$

$$s.t.: \quad pflow(p_t^{\mathcal{G}}, q_t^{\mathcal{G}}, p_t^{\mathcal{L}}, q_t^{\mathcal{L}}, v_t, i_t^{xfm}) = 0, \quad (6)$$

$$\underline{p_t^{\mathcal{G}}} \le p_t^{\mathcal{G}} \le \overline{p_t^{\mathcal{G}}}, \underline{q_t^{\mathcal{G}}} \le q_t^{\mathcal{G}} \le \overline{q_t^{\mathcal{G}}}, \quad (7)$$

$$\underline{v} \le v_t \le \overline{v}, \underline{i_{xfm}} \le i_t^{xfm} \le \overline{i_{xfm}}, \quad (8)$$

where $f(x_t)$ represents the objective. It is adapted to the system operational mode and will be explained in the following subsections. v_t, i_t^{xfm} denote the system nodal voltage and transformer loading, and $\underline{v}, \underline{i_{xfm}}$ and $\overline{v}, \overline{i_{xfm}}$ are the lower and upper limits, respectively. Equations (6)-(8) represents power flow equations, DER operational constraints, and system security constraints. Recognizing that constraints (6) are nonlinear, the OPF (5)-(8) is a nonconvex, nonlinear, NP-hard programming problem, which suffers from high computational complexity. Furthermore, constraints (6) also require an accurate system model and load request profile along the whole scheduling horizon, which are hard to acquire in real world.

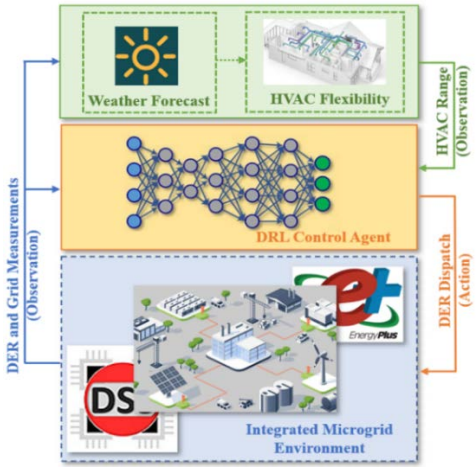

Fig. 2. Scheme of the DRL-based microgrid management.

Therefore, this paper proposes a deep reinforcement learning (DRL)-based solution, as shown in Fig. 2. The microgrid and building simulation model, created by a co-simulation between OpenDSS distribution system model and a data-driven building model derived from EnergyPlus simulation, serves as the integrated environment. From the environment, measurements of DER components and grid will be collected and sent to DRL as observations. The building temperature and weather data, as discussed in Section II, will be delivered to the flexibility estimation module to obtain the HVAC controllable power range, which are also treated as the observation to the DRL controller. DRL will next provide the dispatch signals to DERs as the action. With the proposed approach, the objective is modeled as the reward function. The power flow constraints (6) and the building temperature variation are enforced in the integrated microgrid environment. Violations of constraints (8) are captured by penalty terms to the reward. Constraints (7) are enforced by the DRL control action space [6]. It worth to note that the proposed approach refines the control policy by analyzing and training from historical data, thus reducing the dependency on the distribution system power flow model. Once the training of the control policy is complete, it facilitates near-real-time decision making, aligning with the rapid rates of advanced sensing communications and thereby empowering seamless online applications. In addition, different objectives

(reward functions) and the corresponding observations/action settings will be switched between two different microgrid operational modes. More details about the reward setup are explained in the following subsections.

B. Grid-Connected Operation to Reduce Energy Cost

In the context of the grid-connected operation mode, the goal of controlling DERs is to minimize total energy cost of the microgrid including the cost of purchasing electricity from utility grid based on total kWh energy consumption, the cost of using on-site generators based on total kWh energy, the on-peak demand charge, and the non-coincident demand charge. While solving the minimization optimization problem, the building occupancy comfort should be always satisfied.

This is primarily achieved through the following strategies: (i). Leverage HVAC load flexibility: the HVAC load flexibility information acquired from individual buildings is first adopted. At each time step, the power consumption of HVAC load is constrained by three values: an upper bound $\overline{PL_h^t}$, a lower bound $\underline{PL_h^t}$, and a preferred power consumption $P_{h,pre}^t$. The building occupancy comfort is satisfied by ensuring the actual power consumption of each controllable HVAC load within the flexibility range and as close as possible to the preferred value. (ii). Control of generators: we consider three types of generators including landfill gas, natural gas, and diesel generators. Their respective generation capacities at any given time are denoted as $[P_{lf}^t, P_{ng}^t, P_{dg}^t]$. The generators are used to provide electricity to the loads inside the microgrid with different types and costs.

To calculate the generator cost, three key information are required, including fuel energy contents, generator efficiency, and cost of generator fuel. According to the U.S. Energy Information Administration, the natural gas has 1,000,039 British thermal units (BTU) per 1000 cubic feet. The Diesel has 137,381 BTU per gallon. The landfill gas has a value of 350-600 BTU per cubic foot. The generator fuel efficiency means what percentage of the fuel heat content can be converted to electricity. The gas generator has 19% efficiency, and diesel generator has 27% efficiency. The diesel generator cost per kWh can be calculated to be \$0.34 and the natural gas generator cost per kWh is \$0.25. Nevertheless, the complexity of landfill gas components presents a challenge in cost calculation. The generator's efficiency is difficult to determine due to the variable composition of landfill gas. Based on [7], an annual summary report on landfill gas generation in Canada, the cost per kilowatt-hour for a landfill gas generator stands at \$0.19.

In addition, on-peak demand charge and non-coincident demand charge are considered when calculating the total energy cost. The on-peak demand charge is based on the highest amount of power used by the customer at any single point during the billing period, but specifically during the peak hours when the demand for electricity in the grid is at its highest. In this paper, we consider the peak hour as from 4 p.m. to 9 p.m., and the on-peak demand charge price is \$15.89/kW. Non-coincident demand charge refers to the highest rate of electricity usage by a customer. This charge is a fee based on the maximum amount of power the customer used at any single point during a billing period, regardless of whether it coincides with the system's peak demand. In this paper, the non-coincident demand charge price is set to \$19.12 per kW.

To address this problem using DRL, we formulated a Markov decision process (MDP) in which the observation and action spaces are defined as:

- **Observation** $\boldsymbol{o_t} \coloneqq [p_{\mathcal{H}}^t, p_{\mathcal{L}}^t, p_{\mathcal{FH},l}^t, p_{\mathcal{FH},u}^t, p_{\mathcal{FH},pre}^t]^\intercal$, which includes PV inverters generation $p_{\mathcal{H}}^t$, non-controllable load $p_{\mathcal{L}}^t$, flexible HVAC upper, lower, and preferred power bound $[p_{\mathcal{L}}^t, p_{\mathcal{FH},l}^t, p_{\mathcal{FH},u}^t, p_{\mathcal{FH},pre}^t]$.
- **Action** $\boldsymbol{a}_t \coloneqq [P_t^{lf}, P_t^{ng}, P_t^{dg}, PL_h^t]^\intercal$: The action at timestep t includes the dispatch of three different types of generators; and flexible HVAC active power setpoints.

In addition, for objective/reward function, since the non-coincident charge is only incurred at the end of the week in this problem, it represents a sparse reward for DRL. If directly included in the reward function, it could negatively impact the training process. Given that the essence of the non-coincident charge is to reduce the demand on the main grid, we introduce a threshold μ in the reward function to decrease the power demand from the main grid by the microgrid. The objective/ reward function is modified as following:

$$r_t = -C_{\mathrm{t}}^{utilites} - C_{\mathrm{t}}^{\mathcal{D}} - \mathcal{FH}_{\mathrm{t}}^{\mathcal{D}diff} - pen, \tag{9}$$

$$pen = \sigma \times C_{\mathrm{t}}^{utilites}, if\ P_{demand}^t \geq \mu, \tag{10}$$

where σ is coefficient of penalty when the power demand from main grid is higher than threshold μ.

C. Islanded Operation to Improve Resilience

During islanded microgrid operation mode, a prioritized critical load restoration (CLR) problem after a microgrid gets islanded due to the substation outage is investigated. Loads $i \in \mathcal{L}$ are prioritized by importance factors $\mathscr{b}^i$, and $\boldsymbol{z} = [\mathscr{b}^1, \dots, \mathscr{b}^N]$, $N = |\mathcal{L}|_1$. To solve this problem, the following assumptions are made: (i) Available energy for $\mathcal{G}$ are limited. (ii) The length of restoration horizon/substation repair time $\mathcal{T}$ is deterministic and known when restoration starts. (iii) Loads $\mathcal{L}$ can be partially restored with the same power factor, i.e., $x_t \coloneqq (p_t^{\mathcal{G}}, q_t^{\mathcal{G}}, p_t^{\mathcal{L}}, q_t^{\mathcal{L}})$, (iv) Grid topology is assumed to be intact, and we defer the inclusion of topology restoration to our future work.

For objective/reward function, at each control step $t \in \mathcal{T}$, the power setpoints of DERs are dynamically determined in order to maximize the following:

$$f(x_t) = C_t^{CLR} - C_t^{VV} - C_t^{XFR} \tag{11}$$

where

$$C_t^{LR} = z^\top p_t^{\mathcal{L}} - z^\top diag\{\epsilon\}\left[p_{t-1}^{\mathcal{L}} - p_t^{\mathcal{L}}\right]^+, \tag{12}$$

$$C_t^{VV} = \lambda 1_{N_b}^\top \mathrm{diag}\{\delta v_t\}\delta v_t, \tag{13}$$

$$\delta v_t = [v_t - \overline{v}]^+ + [\underline{v} - v_t]^+ \tag{14}$$

$$C_t^{XFR} = \lambda 1_{N_{xfr}}^\top \mathrm{diag}\{\delta i_t^{xfm}\}\delta i_t^{xfm} \tag{15}$$

$$\delta i_t^{xfm} = [i_t^{xfm} - \overline{i_{xfm}}]^+ + [\underline{i_{xfm}} - i_t^{xfm}]^+ \tag{16}$$

where C_t^{CLR}, C_t^{VV} and C_t^{XFR} represent the single-step CLR reward, voltage and thermal violation penalty. N_b, N_{xfr} indicates the number of nodes and transformers. In (12), the first term encourages load restoration, and the second term penalizes shedding previously restored by factors of ϵ_c. This penalty facilitates a reliable and monotonic restoration and thus minimizes the impact of intermittent renewable generation. The value of ϵ can be adjusted to manage the strictness of the monotonic load restoration requirement. Specifically, the CLR

controller should only restore load i if it can be sustained for the next $\epsilon_i + 1$ steps to obtain a positive reward. Eq. (13)-(16) penalize the nodal voltage and transformer thermal violations.

For observation and action setup:

- **Observation** $o_t \coloneqq [p_{t,k}^{\mathcal{H}}, e_t^{\mathcal{B}}, e_t^{\mathcal{D}}, p_t^{\mathcal{FH},u}, p_t^{\mathcal{FH},l}, p_t^{\mathcal{L},req}, p_{t-1}^{\mathcal{L}}, t, \phi(t)]^\intercal$, which include the available PV power forecasts for k steps look-ahead period $p_{t,k}^{\mathcal{H}}$; the state of charge (SOC) of all batteries $e_t^{\mathcal{B}}$; the remaining fuel of generators $e_t^{\mathcal{D}}$; flexible HVAC load upper and lower bounds $p_t^{\mathcal{FH},u}$, $p_t^{\mathcal{FH},l}$; load requests $p_t^{\mathcal{L},req}$; supplied load value from the last time step $p_{t-1}^{\mathcal{L}}$; the step index t, and a natural time coding $\phi(t)$.
- **Action** $\boldsymbol{a}_t \coloneqq [p_t^{\mathcal{H}}, q_t^{\mathcal{H}}, p_t^{\mathcal{B}}, p_t^{\mathcal{D}}, q_t^{\mathcal{D}}, p_t^{\mathcal{FH}}, p_t^{\mathcal{L}}]^\intercal$: The action at step t includes dispatch of PV inverters $p_t^{\mathcal{H}}, q_t^{\mathcal{H}}$; batteries $p_t^{\mathcal{B}}$; generators $p_t^{\mathcal{D}}, q_t^{\mathcal{D}}$; flexible HVAC load $p_t^{\mathcal{FH}}$; and load pickup decisions $p_t^{\mathcal{L}}$.

IV. Case Study

A. Microgrid System Description

To demonstrate the performance of the proposed learning-based building flexibility estimation and control, we implemented simulation tests on the model of a real microgrid located in Southern California. The microgrid consists of 3,744 nodes, including both the primary and secondary nodes. The topology of the microgrid is depicted as Fig. 3. Multiple DERs exist in the microgrid, including 15 PV systems of 1.5 MW, 2 natural gas generators of 2.8 MW, 2 landfill gas generators of 3.2 MW, 39 distributed diesel generators of 10.6 MW, and 1 1.8MW/2MWh battery system.

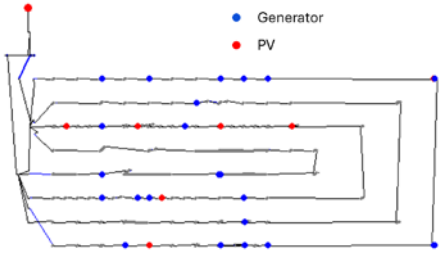

Fig. 3. The topology of the microgrid.

There are 436 buildings in the microgrid. EnergyPlus was employed to simulate time series building load data based on real field information such as building type, size, and local climate conditions. 32 typical building types and geographic data from the microgrid site were used for accurate simulations. Outputs include various load profiles, solar radiation rates, and zonal temperatures, all calculated at 5-minute intervals over a year. Two datasets were produced: one using default HVAC settings for microgrid modeling, and another with random hourly HVAC setpoints between 15 °C and 27 °C for training the data-driven building HVAC flexible load model. The HVAC system activates heating or cooling based on these setpoints. Additionally, buildings with known yearly energy consumption have their load profiles adjusted to align with the field data from the microgrid site, highlighting a peak load of around 12 MW in summer.

B. Simulation Results

(1) Flexibility Analysis

Utilizing the hybrid module in Section II, the HVAC flexibility of each building can be acquired. Fig. 4 shows the flexibility result quantified for one building. At each time stamp, the green line is the upper bound p_u, the blue line is the lower bound p_l, and the black line is the HVAC energy consumption at default temperature setting, which is $22°C$. At peak, the flexibility can be more than 20 kW for this specific building. In addition to the single building HVAC flexibility analysis, we also present the statistical flexibility analysis result of all 32 types of buildings in Fig. 5. As shown, the HVAC consumption ranges from around 1 kW to up to 300 kW, with most of them ranging from several kW to close to 50 kW. The outliers with large flexibility results are caused by three buildings with very large HVAC loads. Also, it can be noted that the flexibility results vary among 12 months, which is caused by time-varying weather conditions.

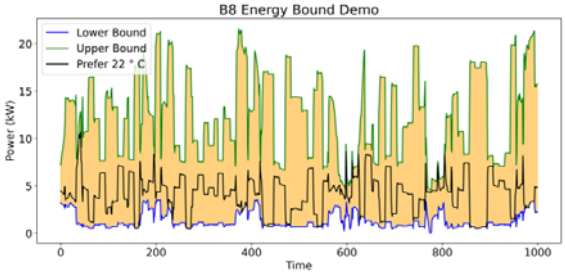

Fig. 4. HVAC flexibility of one building.

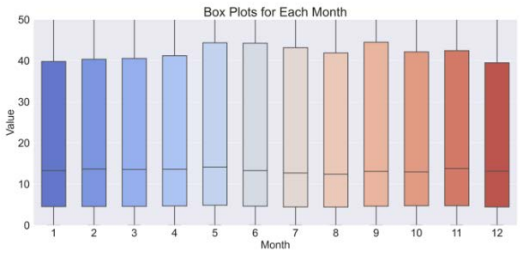

Fig. 5. Boxplot of all 32 building types flexibility analysis.

(2) Grid-Connected Operation

For the grid-connected operation mode, the DRL agent was trained using one-month load information, collected at 15-minute intervals. Following the completion of this training phase, the learned model was use for a 7-day simulation test.

The result of the power demand from the main grid is shown in Fig. 6. For the baseline when there is no control, the peak load demand reaches to 8904 kW, occurring at the 540th time step, corresponding to the afternoon of the sixth day. However, with the application of the proposed DRL control over the generator operations, this demand decreases to 4,111 kW. After considering the HVAC flexibility, this demand is further reduced to 3,667kW. The total energy consumption supplied from the grid over the entire 7 days was also calculated and compared: the baseline result is 739,046 kWh, the DRL control without considering HVAC flexibility result is 488,618 kWh, and the DRL control considering HVAC flexibility is 458,583 kWh. The energy bill cost was then calculated by following III.B and the result was shown in Table I. From these. results, the overall effectiveness of the DRL control with flexibility

information incorporated on reducing microgrid energy cost is well proved.

Fig. 6. Microgrid head load during grid-connected opeartion.

Table. I. Energy bill comparison ($)

	Baseline	DRL w/o. flex.	DRL w. flex.
On-peak charge	94,171	59,159	54,688
Non-coin. charge	170,195	78,603	70,126
Generator cost	-	77,942	78,015
Grid purchase cost	59,123	39,089	36,686
Total	323489	254793	239515

Fig. 7 illustrates the power consumption pattern of an HVAC system under the control of DRL algorithm is operating within the allowed operation range. During the testing period, if no flexibility, a total of 290,149 kWh of energy would be consumed. However, by incorporating flexibility, the total energy consumption would be 252,882 kWh, which represents a reduction of 12.8% in energy consumption.

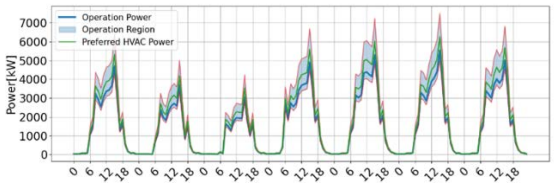

Fig. 7. Onsite generation dispatch during grid-connected operation.

(3) Islanded Microgrid Operation

For islanded operation mode, a CLR problem was also tested using the one week data with 15-min time resolution. The criticalities of total 436 buildings were differentiated by different importance factors, which were defined based on the field load shedding plan. Then, we categorized all the buildings into critical loads with $\mathscr{b} = 1$, flexible HVAC loads with $\mathscr{b} = 0.5$, and non-critical loads with $\mathscr{b} = 0.1$.

The system-wide load restoration curve (with original HVAC load) is depicted in Fig. 8. The blue area is the total supplied load across the system. The red, orange, and dark green curve reports the critical, critical plus flexible, and total (critical plus flexible and noncritical) load request. It can be observed that the developed critical load restoration agent can properly dispatch the on-site generation resources so as to supply all critical load during the 7-day operation. Further, partial of flexible load are also supplied.

To justify the benefit of introducing HVAC flexible load and proposed RL methodology, we implemented the 7-day load restoration problem with proposed solution and compared to the Model Predictive Control (MPC) [2] in Fig. 9. It can be observed that the proposed solution and supply all the critical loads and maintain the supplied facility number around 1,000. While the MPC with 6-hour time window can supply higher load value and facility number for 5 days; however, due to the completed information is not known during the MPC decision process, both load value and facility number drop starting day 6. It can be observed that almost all critical load are even curtailed at the end of 7-day simulation.

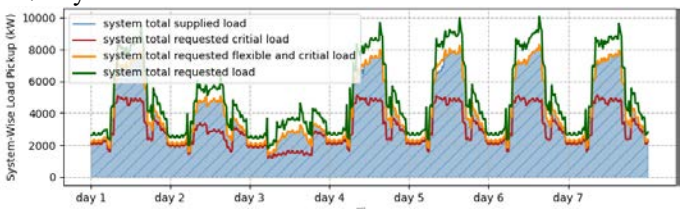

Fig. 8. Microgrid total load supply during islanded operation.

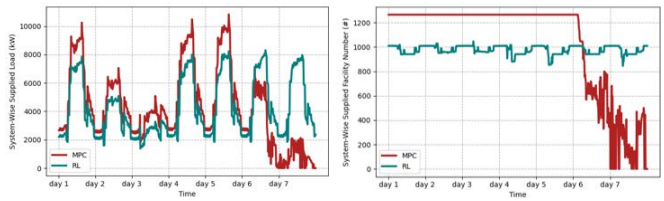

Fig. 9. The number of facility supplied with/without HVAC flexible load.

V. Conclusion

This paper proposed a learning-based building load flexibility estimation and control framework to improve system economics and resilience. Without knowledge of building HVAC load model, we can use historical HVAC load measurements to estimate building load flexibility effectively. The proposed work is demonstrated on a real California microgrid model. Simulation studies have proved that the incorporation of building load flexibility into microgrid control can reduce microgrid system energy cost significantly and also can help improve system resilience by restoring more buildings effectively. This study only considers the building HVAC load flexibility, but our proposed flexibility estimation method and DRL controls can be applied to any type of loads. In the future, we will demonstrate the study by considering other typical types of loads such as residential electric water heaters and electric vehicles.

References

[1] P. Wang, D. Wu, and K. Kalsi, “Flexibility estimation and control of thermostatically controlled loads with lock time for regulation service,” IEEE Trans. Smart Grid, vol. 11, no. 4, July 2020.

[2] W. Liu, F. Ding, “Collaborative distribution system restoration planning and real-time dispatch considering behind-the-meter DERs,” IEEE Trans. Power Syst., vol. 36, no. 4, July 2021.

[3] B. Chen, Z. Ye, C. Chen, J. Wang, “Toward a MILP modeling framework for distribution system restoration,” IEEE Trans. Power Syst., vol. 34, no. 3, May 2019.

[4] Y. Lin, A. Das and Z. Ni, "A Modified Maximum Entropy Inverse Reinforcement Learning Approach for Microgrid Energy Scheduling," in 2023 IEEE Power & Energy Society General Meeting, Orlando, FL, USA, 2023, pp. 1-5.

[5] Y. Gao, S. Li, W. Dong, “A learning-based load, PV and energy storage system control for nearly zero energy building,” in 2023 IEEE Power & Energy Society General Meeting, Orlando, FL, USA, 2023, pp. 1-5.

[6] Y. Yao, X. Zhang, J. Wang and F. Ding, "Multi-Agent Reinforcement Learning for Distribution System Critical Load Restoration," 2023 IEEE Power & Energy Society General Meeting (PESGM), Orlando, FL, USA.

[7] D. Kerr, "2022 Lindsay Ops Landfill Gas Generator Summary," in Committee of the Whole Report, no. WM2023-006, [Kawartha Lakes], Mar. 7, 2023.